Article

Virtual Prototyping of the Cement Transporter Including Strength Criterion Based on Geotechnical Boundary Conditions

Krzysztof Nieśpiałowski [1,*], Jarosław Tokarczyk [1], Sławomir Bartoszek [1], Piotr Kanty [2], Norbert Kurek [2], Andrzej Dymarek [3] and Tomasz Dzitkowski [3]

[1] KOMAG Institute of Mining Technology, Pszczyńska 37, 44-101 Gliwice, Poland; jtokarczyk@komag.eu (J.T.); sbartoszek@komag.eu (S.B.)

[2] Menard Sp. z o.o., Powązkowska 44c, 01-797 Warszawa, Poland; pkanty@menard.pl (P.K.); nkurek@menard.pl (N.K.)

[3] Department of Engineering Processes Automation and Integrated Manufacturing Systems, Silesian University of Technology, Konarskiego 18A, 44-100 Gliwice, Poland; andrzej.dymarek@polsl.pl (A.D.); tomasz.dzitkowski@polsl.pl (T.D.)

[*] Correspondence: kniespialowski@komag.eu; Tel.: +48-32-2374-592

Abstract: Regarding the vehicles used in civil engineering, some are manufactured in large quantities and some (especially innovative ones) are still prototypes manufactured for tests or rare use. The latter describes the case of equipment for mass mixing (mass stabilization) technology which is not widely used compared to other types of geotechnical equipment. The purpose of this paper is to present a research and development project on an innovative cement transporter designed for mass mixing. Three-dimensional models and advanced finite element method (FEM) calculations are used to validate the design of the most important part of the cement transporter—the frame connecting the undercarriage and the upper carriage. The results presented in the paper confirm that the design based on the strength criterion and boundary conditions from geotechnical safety requirements can be used for designing the parts of the prototype vehicle. It is concluded that in innovative vehicle design for geotechnical purposes, the analyses may extend beyond the standard static analyses.

Keywords: mass mixing; geotechnics; cement transporter; computer simulations; finite element method

1. Introduction

Mass mixing, otherwise known as solidification or mass stabilization, is a strengthening technology based on improving the strength properties of the weak subsoil by mixing it with a binding agent. It is usually a subsoil reinforcement reaching only a few meters deep. The purpose of this soil improvement technology is to improve the mechanical and deformation parameters of the natural subsoil. The method consists in introducing a special mixing unit into the subsoil, which destroys the subsoil structure and mixes it with the binding agent pumped at the same time (Figure 1). Classic (dry) solidification consists in mixing the subsoil with a binding agent (e.g., cement, cement-ash mixtures) without additional water. This treatment, applied in most cases on organic soils [1], allows the soil to dry (due to the dehydration process) and then bind.

This technology is used in Scandinavian countries but still is not common in Europe or the US. Recently, this technology has begun to be applied in Poland [2]. Guidelines from Scandinavian design experience are available [3]. For effective soil strengthening, it is necessary to use specialized equipment. The scientific project (Number POIR.01.01.01-00-0184/19) on the design of a self-propelled cement transporter intended for use in this technology is the answer to this need. The research work on the innovative mass mixing system is based on three-dimensional (3D) modeling, analysis, and calculations. Part of the research work carried out within the project is discussed in this article. The design of this type of vehicle used on construction sites should be based on machinery standards [4–6]

and material codes for designing. On the other hand, the environment in which the vehicle will work is unpredictable. Therefore, the analysis is out of the normal scope and additional tests are required.
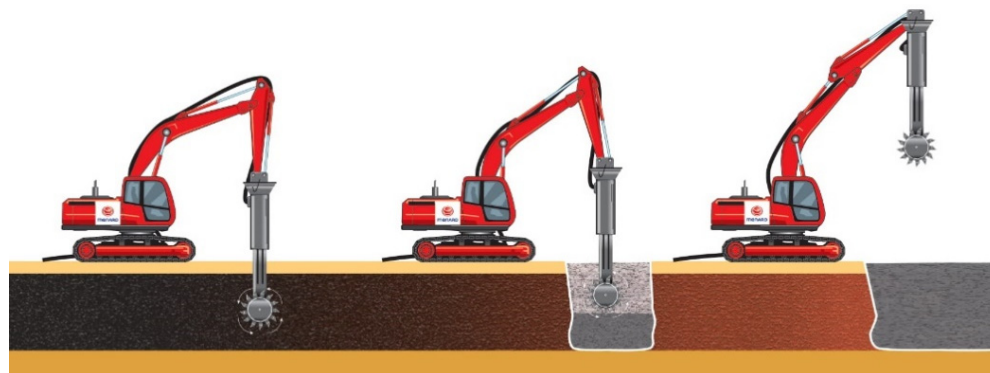
Figure 1. Scheme of soil improvement by the solidification method.

The working platform poses a risk due to its low quality. Methods to avoid the risk are presented in [7–9]. The above-mentioned guidelines show some typical reasons for accidents—mainly a loss of stability/tipping over. The causes of accidents should be eliminated, but at the same time, the design of the equipment should take them into account, and this is the innovativeness of the method presented here. Only the material obstacles, such as hoses full of material, old foundations which were not removed, no densified and highly deformable platform material, and excessive inclination of the working platform, are important. The present work focuses on the two first obstacles. We expect that extended simulations including all aspects will be published later, while tests on the machine–subsoil interaction are still very rare [10,11].

There are two novelties in this solution. First, the system itself (see Figure 2), which contains a cement buffer tank, a transporter, software, and a mixing head—this kind of system does not exist worldwide. The second novelty is the approach to the main component's design (e.g., the frame), where the boundary conditions and analyses are adapted to the design case. The design is not very complicated, but it includes some new aspects of innovation.
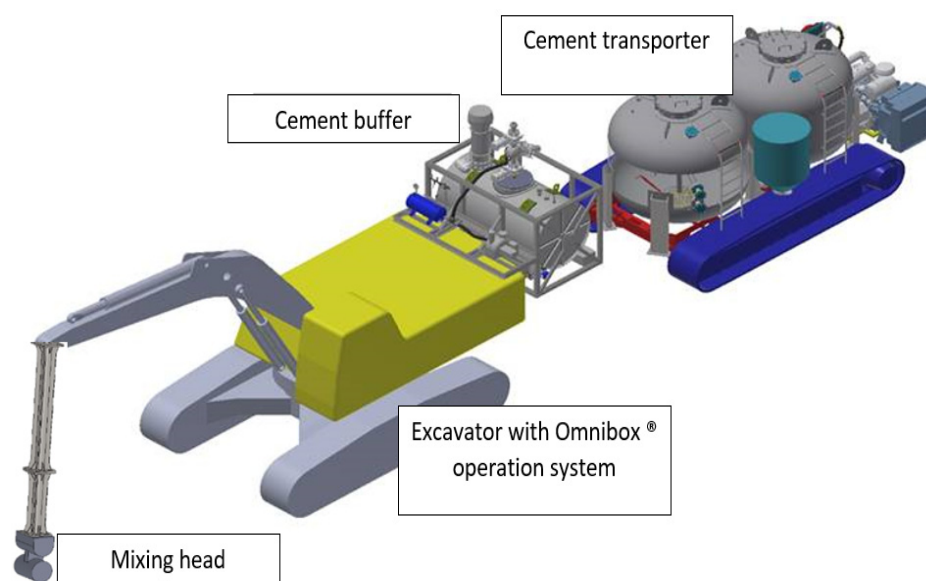
Figure 2. Main mechanical components of soil improvement by solidification.

2. Materials and Methods

2.1. CAD 3D Models

The whole design concept was based on numerical modeling and the possibility to include most of the components as 3D models. The system Omnibox is used for mass mixing (Figure 2) contains a mixing head, an excavator with an operation system able to monitor the soil strengthening parameters [12], a cement buffer tank, and a cement transporter. The paper focuses on the transporter.

Within the transporter, the following components were distinguished: the transporter main frame, crawlers, power unit, control system, and pneumatic components (Figure 3). In addition, the engine frame, compressor frame, and hydraulic equipment frame were designed. This article presents the results of the main vehicle frame numerical calculations (see Section 2.2), where all other components are treated as loads acting on the main frame. Most of them are dead loads, and only cement is treated as a variable load.
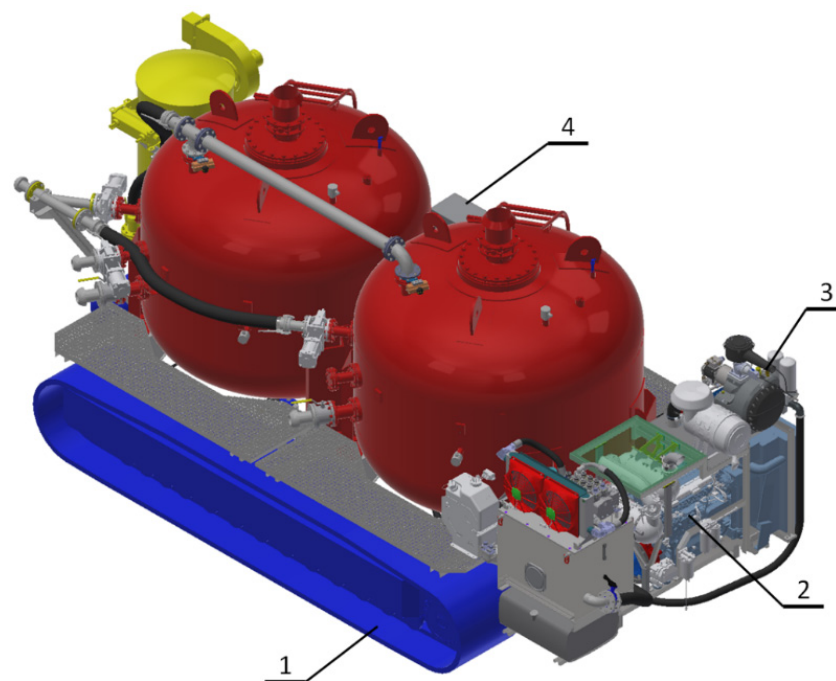
Figure 3. 3D model of the transporter with: 1—crawlers, 2—power unit, 3—pneumatic unit, and 4—control system.

2.2. FEM Computational Models

2.2.1. D Mesh

Based on the 3D geometrical models, computational models were developed in the MSC.Patran (MSC.Software, Santa Ana, CA, USA) [13] software environment, based on the finite elements method (FEM) [14]. Strength calculations were performed in the linear range for static conditions with the use of the MSC.Nastran solver (MSC.Software, Santa Ana, CA, USA) [15]. In the event of dynamic loads, other dedicated solvers were used, e.g., MSC.Dytran (MSC.Software, Santa Ana, CA, USA) [16]. Strength calculations (simulation tests) of the frame assembly of the cement transporter were the research work objective (Figure 4).
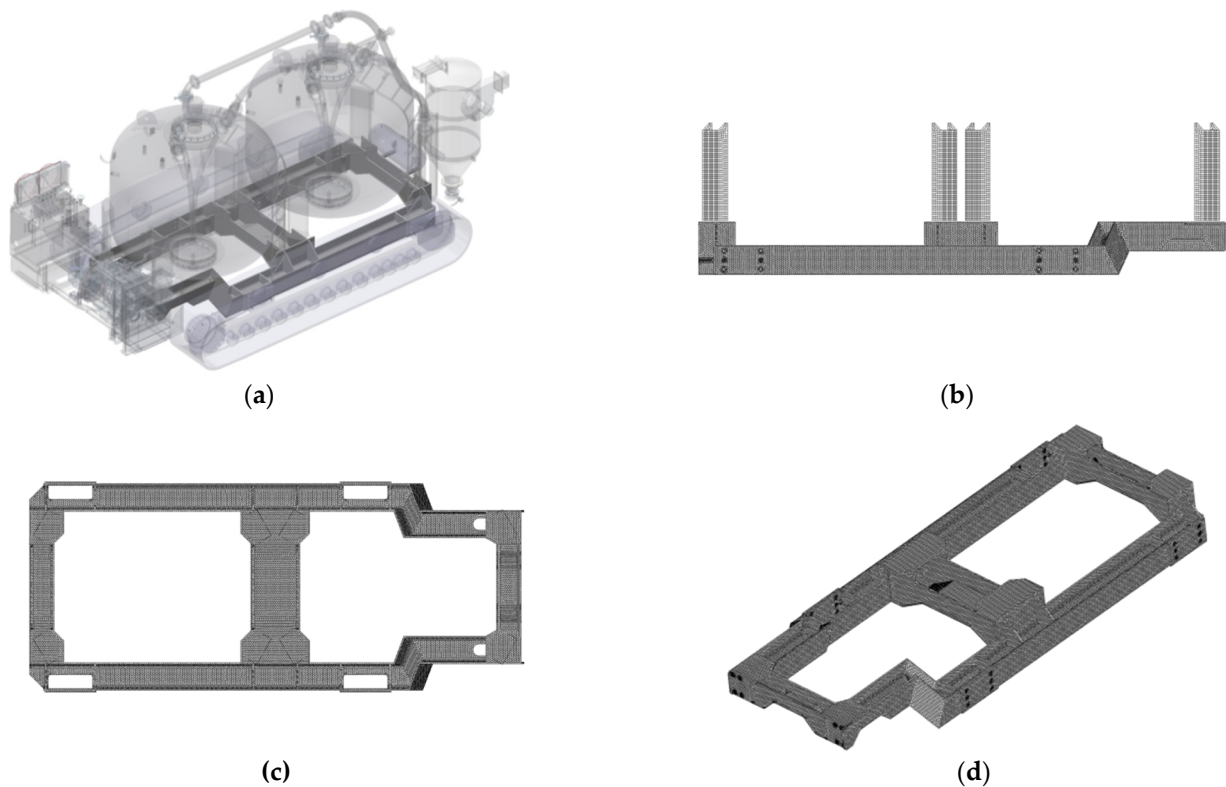
Figure 4. Computational model of the cement transporter main frame: (**a**) position in the transporter, (**b**) side view, (**c**) top view, and (**d**) isometric view.

A spatial geometric model of the frame assembly was discretized using different types of finite elements: second-order tetrahedral solid elements (TETRA10) and shell elements (QUAD4). TETRA10 solid elements ensure high accuracy of calculation results with an acceptable length of calculation time. Their advantage is the ability to discretize complex geometric models [17], which results in their widespread use in structural analyses in different economy branches [18–22].

Apart from the finite element type, the mesh density is another major factor influencing the quality of the obtained calculation results. It has a direct impact on the potential degeneration of finite elements. Therefore, the selection of the size (resolution) of the elements was determined after the verification of the tetrahedral mesh, which consisted of the following stages:

- Aspect: ratio of the height of the element to the square root of the opposing face area.
- Edge angle: the absolute value of the angle between the two faces meeting at an edge, subtracted from $70.529°$.
- Face skew (carried out for each triangular face of the tetrahedral element)—two vectors are constructed: one from a vertex to the mid-point of the opposite edge, and the other between the mid-points of the adjacent edges. The difference results from the angle between these two vectors and $90°$. This procedure is repeated for the other two vertices. The largest of the three computed angles is reported as the skew angle for that element.
- Collapse: An indicator of near-zero volume tetrahedral elements. The test takes the ratio of the height of a vertex to the square root of the area of the opposing face.

2.2.2. Material Model

The following properties of the linear elastic material model were assigned to the steel material in computational models:

- Young modulus, $E = 205$ GPa,

- Poisson's ratio, $\nu = 0.3$,
- Density, $\rho = 7850 \text{ kg/m}^3$.

2.2.3. Boundary Conditions

Three cases of load conditions to the transporter main frame were tested, under normal operating conditions of the cement transporter. These conditions are unfavorable and result in multi-plane torsion of the frame. There were the following cases:

- Case 1—blocking of the left track while the right track drives on. The blocking may occur when old foundations have not been removed from the working platform. Such an obstacle is rigid and will stop the machine. This concerns the criterial state in which the vehicle hits (at a low speed) a non-deformable obstacle on the left side and the drive is activated on the right side. The assumed highest tractive force results from the achieved torque, while not exceeding the permissible values specified by the manufacturer of the drive sprocket (Figure 5).
- Case 2—drive over a convex unevenness such as a hose for pneumatic transport of cement under working pressure. The first track roller is supported on the left side and the penultimate one on the right side. Due to the fact that the vehicle is asymmetrically loaded, it was necessary to carry out a few preliminary numerical calculations in order to find the equilibrium point and select the correct roller that was fixed (Figure 6).
- Case 3—a set of fixations similar to Case 2; however, due to the asymmetrical location of the center of gravity, the first roller on the right and the last roller on the left were supported.

In addition, loads (identical in all variants) related to the mass of the main sub-assemblies were introduced into the computational models. Multi-point constraints were applied, taking into account the object stiffness not included in the computational model. These constraints were also used to connect various types of FEM meshes, e.g., 2D–3D, or were introduced into the computational model in order to dissipate point forces, which may locally generate false stress concentrations (Figure 7).
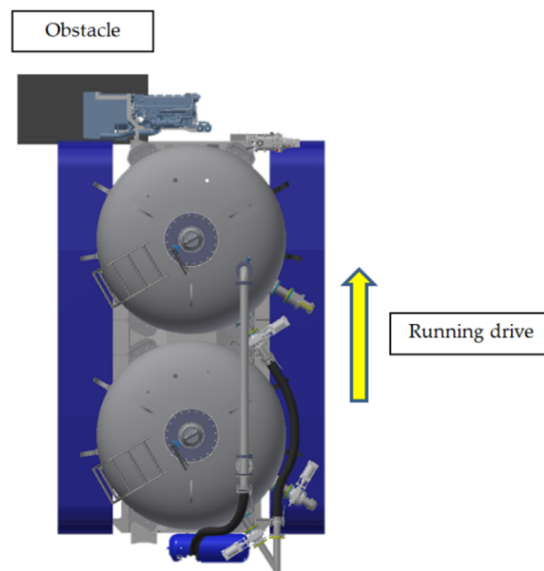
Figure 5. Visualization of the boundary conditions in Case 1.
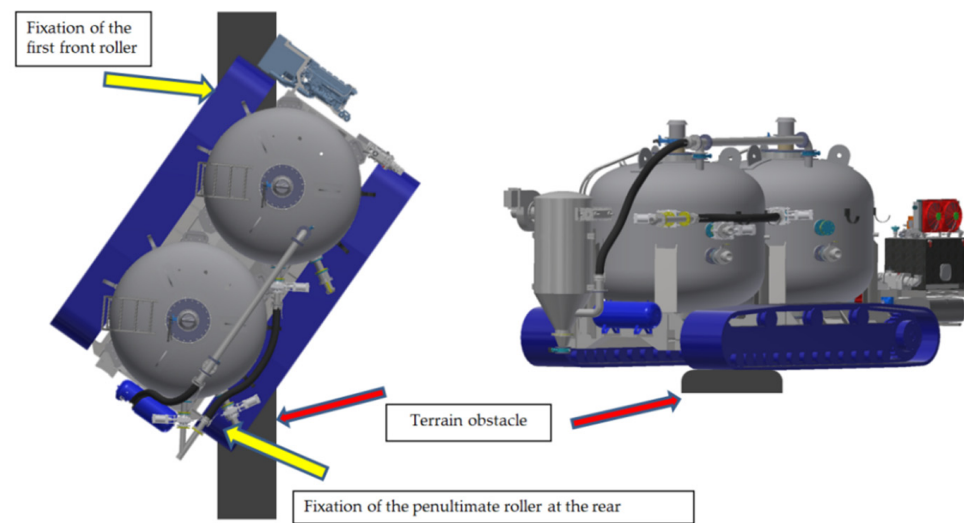
Figure 6. Visualization of the boundary conditions in Case 2.
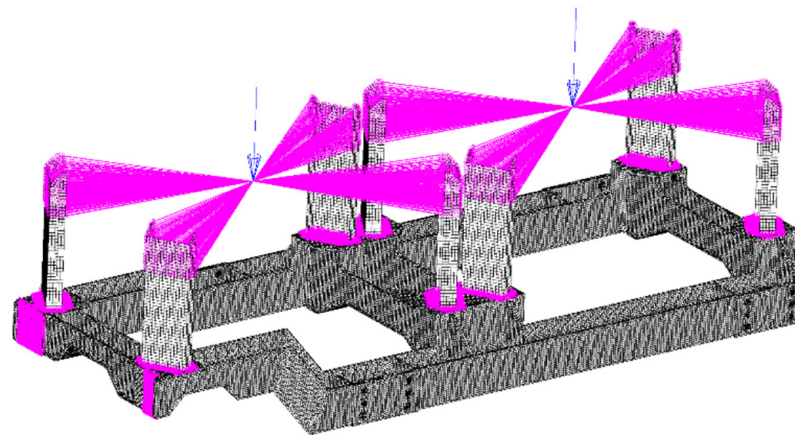
Figure 7. The use of MPC (multi-point constraints) elements during defining the boundary conditions.

The force of gravity was also included in the computational model. It contributed to an increase in reaction time due to the weight of the computational model. Mass was calculated as the quotient of volume and density (solid elements) or as a physical parameter (shell elements). Regarding the other relevant sub-assemblies that impact the load in the main computational model, the superposition method was introduced. That is, the reaction values obtained in previous subtasks were introduced into the computational model with the same magnitude but the opposite direction.

3. Results

The results of the strength calculations for each load variant are presented in the form of maps of displacements, reduced stresses, maximum principal stresses, and iso-surfaces, in Tables 1 and 2. In the presented example, iso-surfaces identified areas (volumes) of the material in which the reduced stresses exceeded the declared value. The stress values are important to design the proper shape of the frame and for verification of used steel. The displacements are important because the deformation of the frame can affect the level of fixation of components such as bulks, engine, compressors, etc. Too high deformations will lead to a risk of separating this part from the frame.

Table 1. Results of numerical strength calculations (maps of displacements and reduced stresses).

Number of Load Case	Displacements	Reduced Stresses
1		
	Maximum value of displacements: 5.58 mm	Maximum value of reduced stresses: ~300 MPa
2		
	Maximum value of displacements: 5.40 mm	Maximum value of reduced stresses: ~200 MPa
3		
	Maximum value of displacements: 5.53 mm	Maximum value of reduced stresses: ~200 MPa
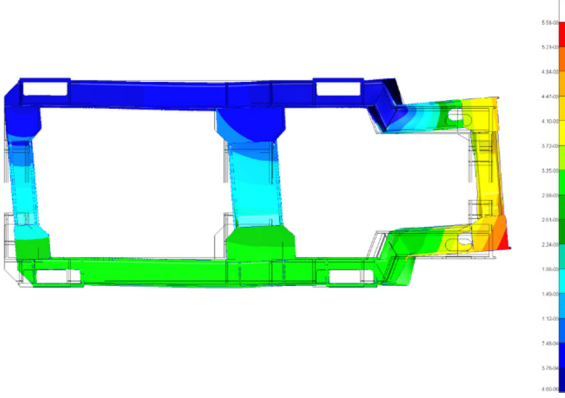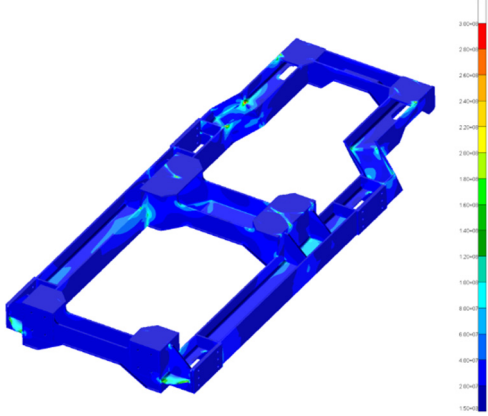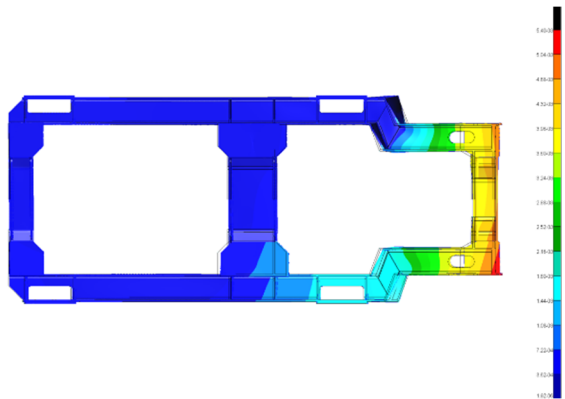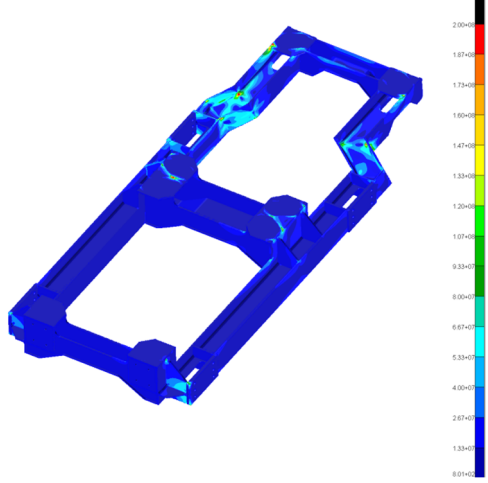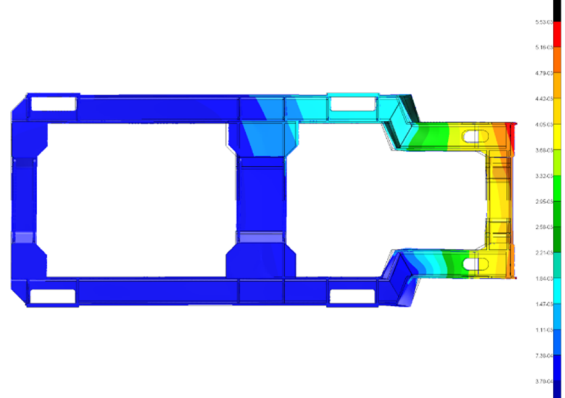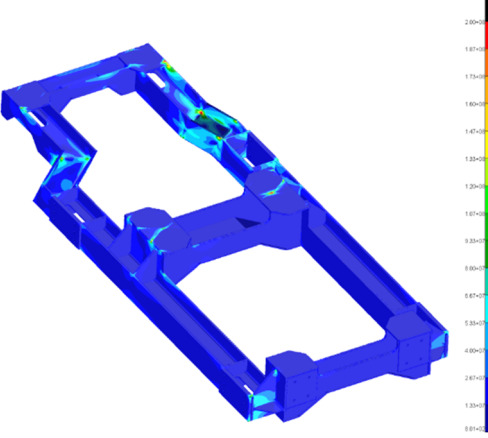
Table 2. Results of numerical strength calculations (maps of maximum principal stresses and iso-surfaces).

Number of Load Case	Maximum Principal Stress	Iso-Surfaces
1	Maximum value of principal stress: 300 MPa	Iso-surface of maximum stresses equal to 100 MPa
2	Maximum value of principal stress: ~200 MPa	Iso-surface of maximum stresses equal to 100 MPa
3	Maximum value of principal stress: ~200 MPa	Iso-surface of maximum stresses equal to 100 MPa
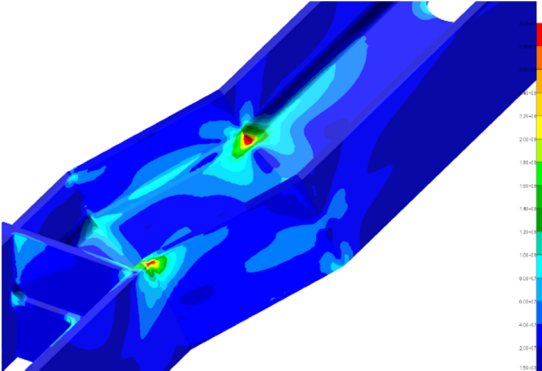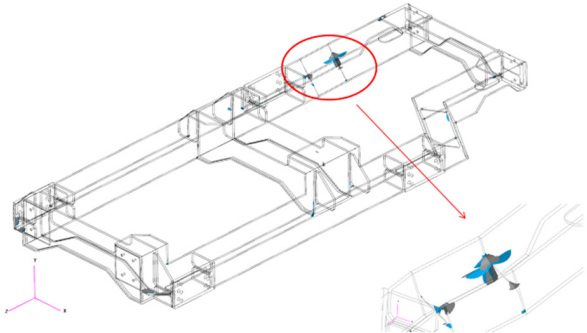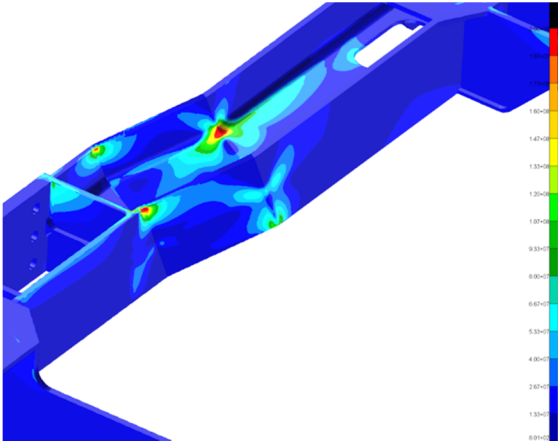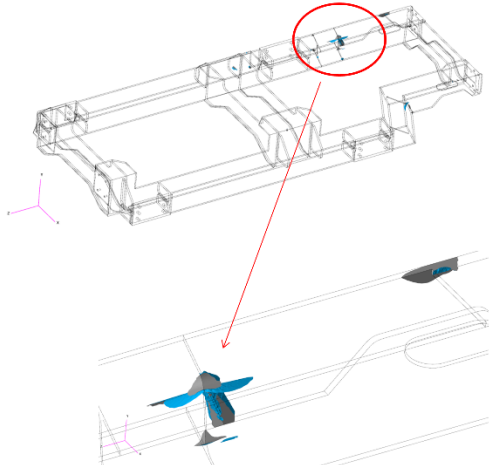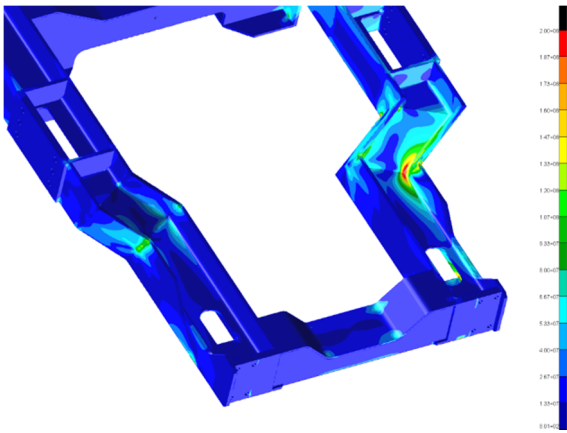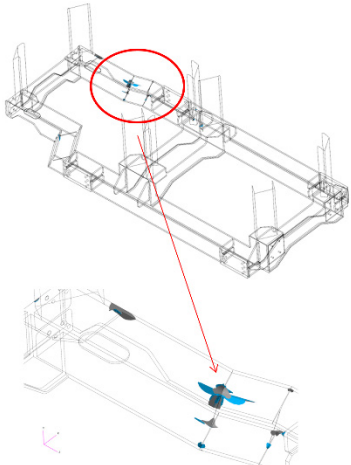
4. Discussion and Conclusions

This article presented the results of the numerical FEM strength calculations of the main frame of the cement transporter based on three cases selected from the geotechnical

practice and current construction site observations. Three different loads, corresponding to the momentary, asymmetric support system of the tracked chassis (crossing an obstacle) and to the blocking of the left side of the undercarriage with the right-track drive, were entered for calculation. These variants, generating frame torsion, were identified as unfavorable.

A detailed description of the three loading cases is presented in Section 2.2.3. Their "disadvantage" was that they require the biggest effort in the main load-carrying sub-assembly, i.e., the vehicle frame. Obviously, other catastrophic scenarios that will cause the vehicle damage may occur, however at this stage, the necessity of increasing the amount of material in the main components of the machine (and simultaneously its weight) should be balanced in relation to the risk of experiencing hypothetical, critical scenarios, e.g., losing stability and tipping over. It should be highlighted that the results of strength calculations were conducted only for static loads, for several reasons. First, in such conditions, it is possible to determine the boundary conditions in detail, in particular a calculation of external loads acting on the vehicle as regards their spot as well as their value. A calculation of dynamic overloads at the design and construction stage involves a lot of uncertainty. A crash into an obstruction can be an example. To calculate an overload acting on the vehicle, it should be taken into account whether the obstruction is at least partly deformable, where exactly the impact happened, if there was a terrain inclination, what the load of the vehicle was like in that particular moment, and what role in the dissipation of the kinetic energy was played by the deforming vehicle equipment that was at the impact point. To calculate the biggest overload, it would be necessary to analyze combinations of the aforementioned cases, which would create a need for constructing many calculation tasks. Another issue is the time-consumption of the dedicated FEM analytical model, the necessity of highly qualified staff and specialist software for quick-changing phenomena (i.e., explicit approach). All of these aspects mean that the issue of taking dynamics into consideration is time-consuming and often impossible to be conducted during a typical design and construction process of a machine. This is why so-called safety factors are used and the obtained maximal values of stresses cannot exceed the determined percentage value, e.g., the yield point of the material.

In the presented case, the obtained results led to strengthening the selected nodes of the construction (an increase of the transverse cross-cut and local use of the material having increased strength parameters).

A proper virtual prototyping process requires from the specialist both basic knowledge in the field of mechanics and experience in creating the computational models. In the case of static or quasi-static analyses, special attention should be paid to the correct definition of boundary conditions, which correspond to different loads, since an error at this stage will significantly affect calculation results and their subsequent interpretation. The boundary conditions should have multi-criteria, according to the geotechnical conditions.

The highest stresses and displacements were found in Case 1, i.e., when the left track was blocked, and the tractive force of the right track was in action. The force corresponds to the maximum torque that can be transmitted by the planetary gear of the drive (70 kNm). The maximum displacement was 5.58 mm, and the reduced and maximum principal stresses were approximately 400 MPa. It should be noted that the highest stress (this applies to all variants) was found in the area of the frame narrowing, at the front of the vehicle (on the upper surfaces of the supporting profiles). However, it is a local stress accumulation, which was visible during the analysis of the propagation of the maximum stress into the material (iso-surfaces). These stresses were reduced by optimizing the components' geometry in the most stressed area. Optimization was based on a global–local method. The local model included the area with the highest stress concentrations and its geometry was modified. Internal forces, which were calculated using the global model, were the boundary conditions. It was an iterative process until the required constraints of the objective function were obtained (determined maximal values of principal stresses).

In Cases 2 and 3, the maximum displacements and stresses were close to each other and did not exceed 300 MPa. Presented load variants are to be considered as accidental

design cases. During typical machine operation, the safety factors should be higher, and all design requirements will be met.

Author Contributions: Conceptualization, N.K.; Methodology, P.K.; Investigation, J.T. and K.N.; Validation, P.K., K.N. and S.B.; Writing—Original Draft Preparation, J.T., P.K. and A.D.; Writing—Review and Editing, N.K., K.N., S.B. and T.D. All authors have read and agreed to the published version of the manuscript.

Institutional Review Board Statement: Not applicable.

Informed Consent Statement: Not applicable.

Data Availability Statement: Data sharing not applicable.

Conflicts of Interest: The authors declare no conflict of interest.

References

1. Jendrysik, K.; Rybak, J. Analysis of numerical model parameters for dry-mixed soil-cement composite with high content of organic matter. *IOP Conf. Ser. Mater. Sci. Eng.* **2020**, *869*, 052007. [CrossRef]
2. Jendrysik, K.; Jończyk, M.; Kanty, P. Mass stabilization as a modern method of substrate strengthening. *Mater. Today Proc.* **2021**, *38*, 2068–2072. [CrossRef]
3. Varius Authors Including BRE. *Design Guide for Soft Soil Stabilization. EuroSoilStab: Development of Design and Construction Methods to Stabilise Soft Organic Soils*; BRE Press: Bracknell, UK, 2002.
4. Directive 2006/42/EC of the European Parliament and of the Council of May 2006 on Machinery and Amending Directive 95/16/EC. Available online: https://eur-lex.europa.eu/legal-content/EN/TXT/?uri=celex%3A32006L0042 (accessed on 20 February 2021).
5. *PN-EN 16228-1:2014-07*; Drilling and Foundation Equipment—Safety—Part 1: Common Requirements. Polish Committee for Standardization: Warsaw, Poland, 2014.
6. *PN-EN 16228-6:2014-07*; Drilling and Foundation Equipment—Safety—Part 6: Jetting, Grouting and Injection Equipment. Polish Committee for Standardization: Warsaw, Poland, 2014.
7. EFFC/DFI. EFFC/DFI Guide to Working Platforms 1st Edition January 2020. Available online: https://www.effc.org/content/uploads/2020/07/EFFC-DFI_Guide_For_Working_Platforms_July2020_Edition_1_LowRes.pdf (accessed on 18 October 2021).
8. BRE. Working Platforms for Tracked Plant: Good Practice Guide to the Design, Installation, Maintenance and Repair of Ground-Supported Working Platforms. Available online: https://www.brebookshop.com/samples/146444.pdf (accessed on 18 October 2021).
9. TWf. Working Platforms Design of Granular Working Platforms for Construction Plant A Guide to Good Practice. Available online: https://www.twforum.org.uk/HigherLogic/System/DownloadDocumentFile.ashx?DocumentFileKey=f74318ff-716b-79a3-f483-77f77a584e05&forceDialog=0 (accessed on 18 October 2021).
10. Urbanski, A.; Richter, M. Stability analysis of drilling rigs moving on a weak subsoil. Selected case studies. *Arch. Civ. Eng.* **2020**, *66*, 303–319. [CrossRef]
11. Urbanski, A.; Richter, M. Stability analysis of heavy machinery moving on weak subsoil. Analytical solution. *Eng. Struct.* **2021**, *241*, 112152. [CrossRef]
12. Bunieski, S.; Quandalle, B. A Practical Example of Data Exchange and Expert System Applied to Ground Improvement Works. In Proceedings of the 3rd International Conference on Information Technology in Geo-Engineering, Guimarães, Portugal, 29 September–2 October 2019.
13. Patran Complete FEA Modeling Solution. Available online: https://www.mscsoftware.com/product/patran (accessed on 6 October 2021).
14. Zienkiewicz, O.C.; Taylor, R.L.; Zhu, J.Z. *The Finite Element Method: Its Basis and Fundamentals*, 7th ed.; Butterworth-Heinemann: Oxford, UK, 2013; ISBN 9781856176330.
15. MSC Nastran Multidisciplinary Structural Analysis. Available online: https://www.mscsoftware.com/product/msc-nastran (accessed on 6 October 2021).
16. Kalita, M.; Tokarczyk, J. Designing and virtual prototyping of the structures protecting the mining machines operators. *Min. Mach.* **2019**, *1*, 3–11. [CrossRef]
17. Alliez, P.; Cohen-Steiner, D.; Yvinec, M.; Desbrun, M. Variational Tetrahedral Meshing. *ACM Trans. Graph.* **2005**, *24*, 617–625. [CrossRef]

18. Ramos, A.; Simões, J.A. Tetrahedral versus hexahedral finite elements in numerical modelling of the proximal femur. *Med. Eng. Phys.* **2006**, *28*, 916–924. [CrossRef] [PubMed]
19. Tadepalli, S.C.; Erdemir, A.; Cavanagh, P.R. Comparison of hexahedral and tetrahedral elements in finite element analysis of the foot and footwear. *J. Biomech.* **2011**, *44*, 2337–2343. [CrossRef] [PubMed]
20. Rolek, J.; Utrata, G. Optimisation of the FE Model Based on the No-Load Test Measurement for Estimating Electromagnetic Parameters of an Induction Motor Equivalent Circuit Including the Rotor Deep-Bar Effect. *Energies* **2021**, *14*, 7562. [CrossRef]
21. Gajewski, T.; Garbowski, T.; Staszak, N.; Kuca, M. Crushing of Double-Walled Corrugated Board and Its Influence on the Load Capacity of Various Boxes. *Energies* **2021**, *14*, 4321. [CrossRef]
22. Chang, S.; Jeon, B.; Kwag, S.; Hahm, D.; Eem, S. Seismic Performance of Piping Systems of Isolated Nuclear Power Plants Determined by Numerical Considerations. *Energies* **2021**, *14*, 4028. [CrossRef]